

Characteristics of hafnium oxide resistance random access memory with different setting compliance current

Yu-Ting Su, Kuan-Chang Chang, Ting-Chang Chang, Tsung-Ming Tsai, Rui Zhang, J. C. Lou, Jung-Hui Chen, Tai-Fa Young, Kai-Huang Chen, Bae-Heng Tseng, Chih-Cheng Shih, Ya-Liang Yang, Min-Chen Chen, Tian-Jian Chu, Chih-Hung Pan, Yong-En Syu, and Simon M. Sze

Citation: [Applied Physics Letters](#) **103**, 163502 (2013); doi: 10.1063/1.4825104

View online: <http://dx.doi.org/10.1063/1.4825104>

View Table of Contents: <http://scitation.aip.org/content/aip/journal/apl/103/16?ver=pdfcov>

Published by the [AIP Publishing](#)

Articles you may be interested in

[Dual operation characteristics of resistance random access memory in indium-gallium-zinc-oxide thin film transistors](#)

Appl. Phys. Lett. **104**, 153501 (2014); 10.1063/1.4871368

[Performance and characteristics of double layer porous silicon oxide resistance random access memory](#)

Appl. Phys. Lett. **102**, 253509 (2013); 10.1063/1.4812474

[Well controlled multiple resistive switching states in the Al local doped HfO₂ resistive random access memory device](#)

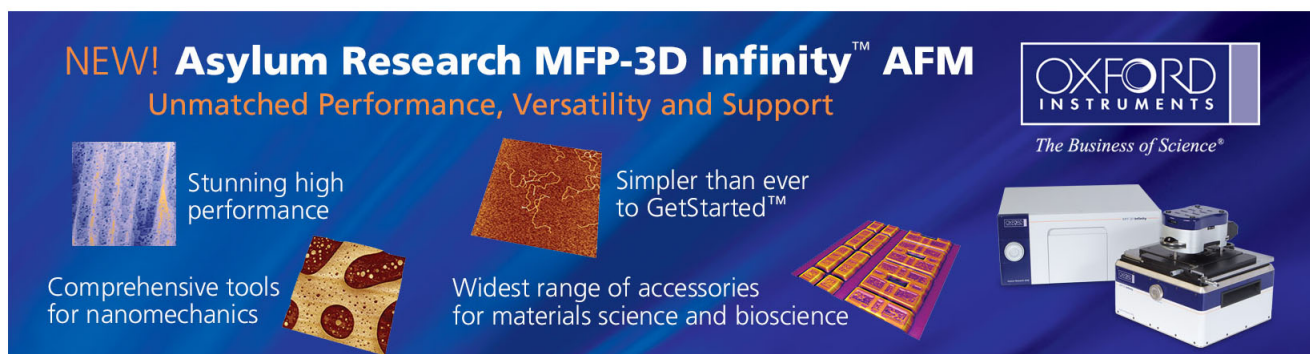
J. Appl. Phys. **113**, 164507 (2013); 10.1063/1.4803076

[Semiconducting-like filament formation in TiN/HfO₂/TiN resistive switching random access memories](#)

Appl. Phys. Lett. **100**, 142102 (2012); 10.1063/1.3696672

[Uncorrelated multiple conductive filament nucleation and rupture in ultra-thin high- dielectric based resistive random access memory](#)

Appl. Phys. Lett. **99**, 093502 (2011); 10.1063/1.3624597

The advertisement features a dark blue background with white and orange text. At the top left, it reads 'NEW! Asylum Research MFP-3D Infinity™ AFM' in large white letters, followed by 'Unmatched Performance, Versatility and Support' in orange. On the right, the Oxford Instruments logo is shown with the tagline 'The Business of Science®'. Below the text are four images: a blue textured surface, a brown textured surface, a yellow and red patterned surface, and a photograph of the AFM instrument. Text boxes describe each image: 'Stunning high performance' (blue), 'Simpler than ever to GetStarted™' (brown), 'Comprehensive tools for nanomechanics' (yellow/red), and 'Widest range of accessories for materials science and bioscience' (yellow/red).

Characteristics of hafnium oxide resistance random access memory with different setting compliance current

Yu-Ting Su,¹ Kuan-Chang Chang,² Ting-Chang Chang,^{1,3,a)} Tsung-Ming Tsai,² Rui Zhang,⁴ J. C. Lou,⁴ Jung-Hui Chen,⁵ Tai-Fa Young,⁶ Kai-Huang Chen,⁷ Bae-Heng Tseng,² Chih-Cheng Shih,² Ya-Liang Yang,⁶ Min-Chen Chen,¹ Tian-Jian Chu,² Chih-Hung Pan,² Yong-En Syu,¹ and Simon M. Sze⁸

¹Department of Physics, National Sun Yat-Sen University, Kaohsiung 80424, Taiwan

²Department of Materials and Optoelectronic Science, National Sun Yat-Sen University, Kaohsiung 80424, Taiwan

³Advanced Optoelectronics Technology Center, National Cheng Kung University, Taiwan

⁴School of Software and Microelectronics, Peking University, Beijing 100871, People's Republic of China

⁵Department of Chemistry, National Kaohsiung Normal University, Kaohsiung, Taiwan

⁶Department of Mechanical and Electro-Mechanical Engineering, National Sun Yat-sen University, Kaohsiung, Taiwan

⁷Department of Electronics Engineering and Computer Science, Tung-Fang Design University, Kaohsiung, Taiwan

⁸Department of Electronics Engineering, National Chiao Tung University, Hsinchu 300, Taiwan

(Received 24 June 2013; accepted 30 September 2013; published online 15 October 2013)

In this Letter, the characteristics of set process of hafnium oxide based resistance random access memory are investigated by different set processes with increasing compliance current. Through current fitting, carrier conduction mechanism of low resistance state changes from hopping to surface scattering and finally to ohmic conduction with the increase of setting compliance current. Experimental data of current-voltage measurement under successive increasing temperature confirms the conduction mechanism transition. A model of filament growth is eventually proposed in a way by merging discrete metal precipitates and electrical field simulation by COMSOL Multiphysics further clarifies the properties of filament growth process. © 2013 AIP Publishing LLC. [<http://dx.doi.org/10.1063/1.4825104>]

Conventional nonvolatile floating memory is expected to reach certain technical and physical limits in the future. Alternative memories have been extensively investigated and among different non-volatile memory (NVM), resistance random access memory (RRAM) has attracted great attention in next-generation NVMs applications owing to the advantages of low operating power, fast operation speed, and high density integration.^{1–12} Researchers have done a lot of research on RRAM including ways to modify its characteristics.^{13–21}

The formation and rupture of filament are considered to be the reason of resistance switching process in resistance random access memory.^{22,23} However, the instantaneous resistance switching is so fast that transcends the measurement capability of modern instruments.

In our research, single layer hafnium oxide^{7,18} by ALD (atomic layer deposition) was deposited to work as the RRAM resistance switching layer. Different set processes with increasing current compliance (C.C.) were applied so as to analyze its characteristics. Conduction current fitting together with vary-temperature current-voltage measurement data were thoroughly investigated, from which conduction filament model was proposed. Finally, COMSOL Multiphysics was applied to simulate electrical field distribution under different set processes with vary current compliance. In order to further confirm the device properties, endurance and retention tests are also conducted.

First, a 200 nm TiN bottom electrode was deposited by using RF sputter. Second, lithography process was taken to

pattern the cell size via. After that, dielectric layer with a thickness of 10 nm was grown using the ALD process. Finally, TiN/Ti layer was sputtered with a thickness proportion of 40 nm/50 nm as our top electrode and acetone was used to etch the photo resistor. The cell size of RRAM devices in this experiment is $0.24 \mu\text{m} \times 0.24 \mu\text{m}$.

The entire electrical measurements of devices were performed using Agilent B1500 semiconductor parameter analyzer.

Before standard current-voltage measurement, an electroforming process was required to activate all of the RRAM devices. Afterwards, DC sweeping was applied to investigate RRAM resistance switching properties.²⁴ In our experiment, we mainly focused on the set process and in order to analyze its characteristics, different set processes with increasing current compliance were employed. Different set processes with C.C. of $50 \mu\text{A}$, $200 \mu\text{A}$, $400 \mu\text{A}$, and the corresponding low resistance state (LRS) current fitting were shown in Figure 1(a). Through conduction current fitting, a noticeable transition of carrier conduction mechanism was found, which gradually changed from hopping conduction to surface scattering and finally to ohmic conduction with the increase of compliance current.

To testify the validity of fitting, vary-temperature I-V measurement was applied and the results were shown in Figure 2. The C.C. for Figures 2(a)–2(c) were $50 \mu\text{A}$, $400 \mu\text{A}$, and $200 \mu\text{A}$, respectively. It can be observed from the experimental data that the current of (a) was directly proportional to temperature while the current of (b) was the opposite. And the current of (c) was independent of temperature. All the

^{a)}Electronic mail: tcchang@mail.phys.nsysu.edu.tw

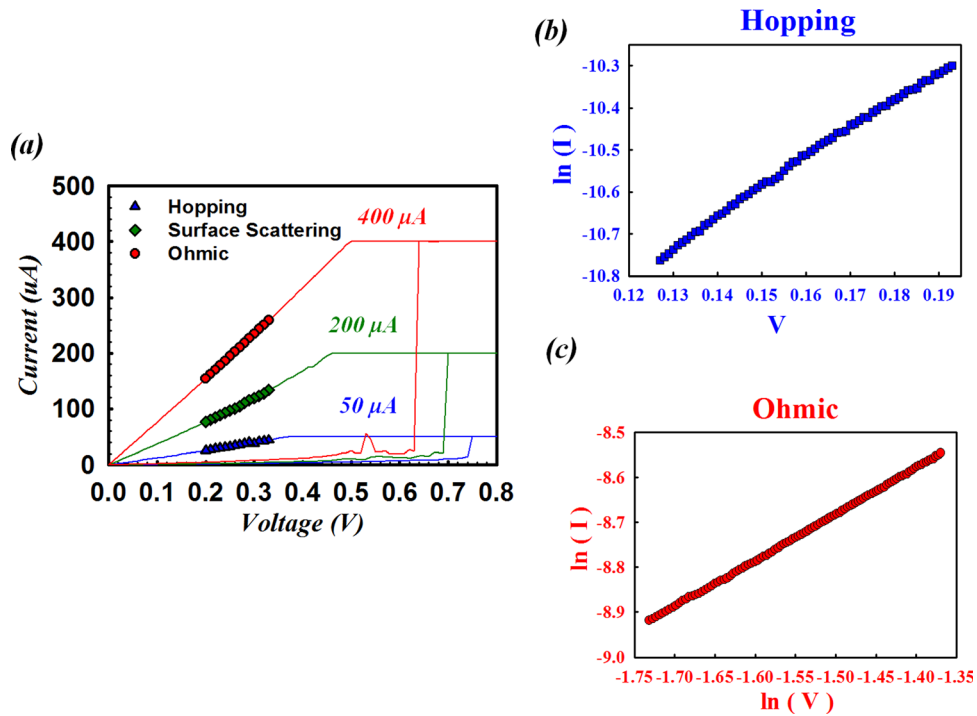


FIG. 1. (a) Current conduction mechanism fitting of LRS with different set current compliance. (b) and (c) are the hopping and ohmic current fitting, respectively.

experimental data were in accordance with their corresponding conduction mechanism.

From the experimental results, a conduction filament model of set process was proposed (Figure 3). As the intensity of current was the main reason for the soft break down of switching dielectric layer, it is easier to break down the dielectric with the increase of conduction current intensity. Thus, denser metal ions would accumulate to form conduction filaments. A current compliance of 50 μA was not strong enough to form continuous filament, which resulted in carrier hopping conduction owing to the discrete metal precipitates (Figure 3(a)). With the intensity increasing of compliance current, the density of metal precipitates will rise and it

became easier for those discrete metal dots to join and merge with each other, from which relative complete filaments can be formed, as shown in Figure 3(b). Because of the formation of smoother carrier conduction path and the independence of temperature, the carrier conduction mechanism transformed from hopping conduction to surface scattering (Figure 1(b)). But the filament is not thick enough for numerous carriers to conduct through, which leads to the crowding of carriers. And the carriers have to force out from the restricted filament which is also the reason why we can find space scattering conduction.²⁵ Meanwhile, measurement result of Figure 2(c) also complies with surface scattering mechanism as current is independent with temperature. If the

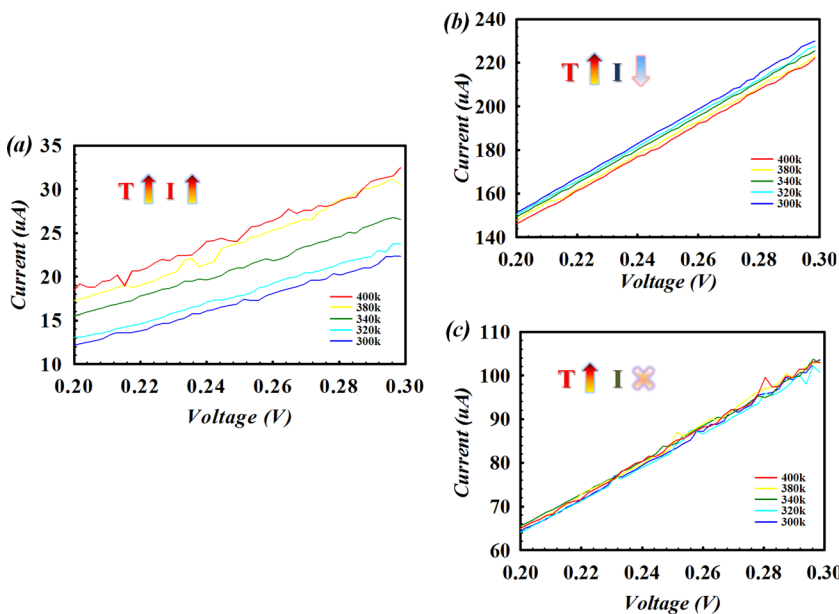


FIG. 2. (a)–(c) are the I–V characteristics of LRS measured under increasing temperature environment. The current compliance of set process for (a), (b), and (c) is 50 μA , 400 μA , and 200 μA , respectively.

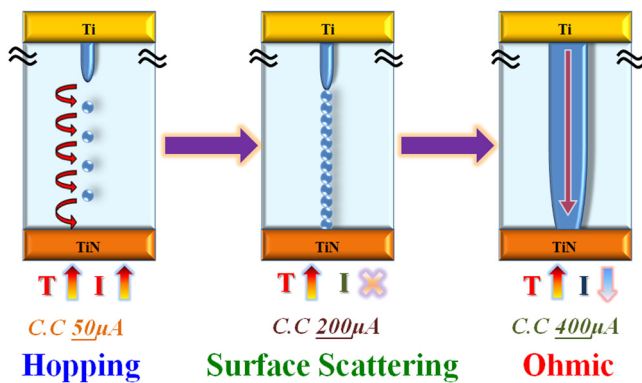


FIG. 3. Gradual merging of precipitates accompanied with transition of conduction mechanism by different set process with increasing current compliance.

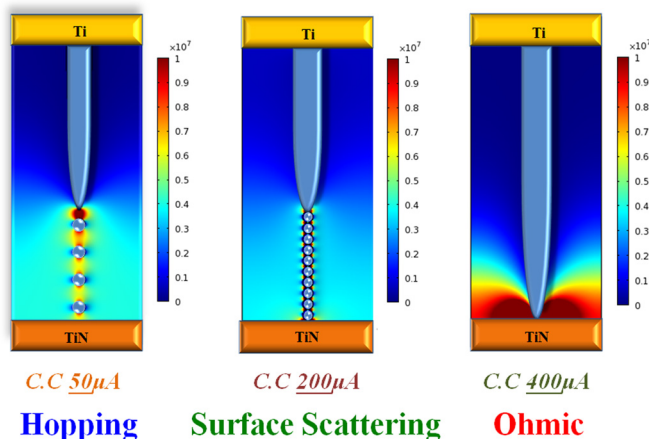


FIG. 4. Electrical field simulation within RRAM switching area.

C.C. further rises to $400\ \mu\text{A}$, ohmic conduction mechanism will dominate due to the formation of thicker and more continuous filament (Figure 3(c)). And the fitting result of ohmic conduction is shown in Figure 1(c).

To better understand the mechanism of filament growth with different C.C., we utilize COMSOL Multiphysics software to simulate the distribution of electrical field. From Figure 4, it can be obviously seen that there exists higher density of electrical field around the tip of metal filament and the area of micro-metal precipitates in dielectric layer. Thus, under small C.C. condition, carriers will hop through those discrete precipitates. While with the increase of C.C., the density of metal precipitates will increase and the electrical field around the vicinity of the precipitates will rise. Thus, there exists more possibility for discrete metal precipitates merging together to form relative more complete filament. But as the filament is not very thick, carriers will be restricted, leading to the surface scattering. If the C.C. of set process is big enough, complete and stable filament will form. And that is also the reason why we can observe ohmic conduction phenomenon.

As endurance and retention properties are basic requirements for non-volatile memories, we have also carried out the tests to confirm the performance and stability for the

multi-state behavior (not shown here). During more than 1000 cycling tests, resistance window remains stable without observing any degradation, and to the retention characteristics the four resistance states reveal good stability.

In conclusion, set process with different current compliance is thoroughly investigated. With the increase of C.C., the conduction mechanism transforms from hopping conduction to surface scattering and finally to ohmic conduction. The transition of carrier conduction mechanism is explained by our model, from which instantaneous resistance switching and filament growth process can be better understood. COMSOL Multiphysics is used to simulate the distribution of electrical field together with the corroboration for endurance and retention tests, which also confirms the phenomenon of discrete metal precipitates merging process.

This work was performed at National Science Council Core Facilities Laboratory for Nano-Science and Nano-Technology in Kaohsiung-Pingtung area and supported by the National Science Council of the Republic of China under Contract Nos. NSC 102-2120-M-110-001 and NSC 101-2221-E-110-044-MY3.

¹M. Wuttig and N. Yamada, *Nature Mater.* **6**, 824–832 (2007).

²T. M. Tsai, K. C. Chang, T. C. Chang, Y. E. Syu, S. L. Chuang, G. W. Chang, G. R. Liu, M. C. Chen, H. C. Huang, S. K. Liu *et al.*, *IEEE Electron Device Lett.* **33**(12), 1696–1698 (2012).

³Q. Liu, S. B. Long, W. Wang, Q. Y. Zuo, S. Zhang, J. N. Chen, and M. Liu, *IEEE Electron Device Lett.* **30**(12), 1335–1337 (2009).

⁴T. C. Chang, F. Y. Jian, S. C. Chen, and Y. T. Tsai, *Mater. Today* **14**(12), 608–615 (2011).

⁵Y. E. Syu, T. C. Chang, T. M. Tsai, Y. C. Hung, K. C. Chang, M. J. Tsai, M. J. Kao, and S. M. Sze, *IEEE Electron Device Lett.* **32**(4), 545–547 (2011).

⁶K. C. Chang, T. M. Tsai, T. C. Chang, Y. E. Syu, S. L. Chuang, C. H. Li, D. S. Gan, and S. M. Sze, *Electrochem. Solid-State Lett.* **15**(3), H65–H68 (2012).

⁷Y. Wang, Q. Liu, S. B. Long, W. Wang, Q. Wang, M. H. Zhang, S. Zhang, Y. T. Li, Q. Y. Zuo, J. H. Yang, and M. Liu, *Nanotechnology* **21**, 045202 (2010).

⁸T. M. Tsai, K. C. Chang, R. Zhang, T. C. Chang, J. C. Lou, J. H. Chen, T. F. Young, B. H. Tseng, C. C. Shih, Y. C. Pan *et al.*, *Appl. Phys. Lett.* **102**, 253509 (2013).

⁹K. C. Chang, T. M. Tsai, T. C. Chang, H. H. Wu, J. H. Chen, Y. E. Syu, G. W. Chang, T. J. Chu, G. R. Liu, Y. T. Su *et al.*, *IEEE Electron Device Lett.* **34**(3), 399–401 (2013).

¹⁰K. C. Chang, R. Zhang, T. C. Chang, T. M. Tsai, J. C. Lou, J. H. Chen, T. F. Young, M. C. Chen, Y. L. Yang, Y. C. Pan *et al.*, *IEEE Electron Device Lett.* **34**(5), 677–679 (2013).

¹¹T. J. Chu, T. C. Chang, T. M. Tsai, H. H. Wu, J. H. Chen, K. C. Chang, T. F. Young, K. H. Chen, Y. E. Syu, G. W. Chang *et al.*, *IEEE Electron Device Lett.* **34**(4), 502–504 (2013).

¹²Y. E. Syu, T. C. Chang, J. H. Lou, T. M. Tsai, K. C. Chang, M. J. Tsai, Y. L. Wang, M. Liu, and Simon M. Sze, *Appl. Phys. Lett.* **102**, 172903 (2013).

¹³K. C. Chang, T. M. Tsai, T. C. Chang, H. H. Wu, K. H. Chen, J. H. Chen, T. F. Young, T. J. Chu, J. Y. Chen, C. H. Pan *et al.*, *IEEE Electron Device Lett.* **34**(4), 511–513 (2013).

¹⁴K. C. Chang, T. M. Tsai, R. Zhang, T. C. Chang, K. H. Chen, J. H. Chen, T. F. Young, J. C. Lou, T. J. Chu, C. C. Shih *et al.*, *Appl. Phys. Lett.* **103**, 083509 (2013).

¹⁵T. M. Tsai, K. C. Chang, T. C. Chang, Y. E. Syu, K. H. Liao, B. H. Tseng, and S. M. Sze, *Appl. Phys. Lett.* **101**, 112906 (2012).

¹⁶K. C. Chang, C. H. Pan, T. C. Chang, T. M. Tsai, R. Zhang, J. C. Lou, T. F. Young, J. H. Chen, C. C. Shih, T. J. Chu *et al.*, *IEEE Electron Device Lett.* **34**(5), 617–619 (2013).

¹⁷Y. Li, S. B. Long, M. H. Zhang, Q. Liu, L. B. Shao, S. Zhang, Y. Wang, Q. Y. Zuo, S. Liu, and M. Liu, *IEEE Electron Device Lett.* **31**(2), 117–119 (2010).

- ¹⁸C. T. Tsai, T. C. Chang, P. T. Liu, P. Y. Yang, Y. C. Kuo, K. T. Kin, P. L. Chang, and F. S. Huang, *Appl. Phys. Lett.* **91**(1), 012109 (2007).
- ¹⁹T. Bertaud, M. Sowinska, D. Walczyk, S. Thiess, A. Gloskovskii, C. Walczyk, and T. Schroeder, *Appl. Phys. Lett.* **101**, 143501 (2012).
- ²⁰M. C. Chen, T. C. Chang, S. Y. Huang, K. C. Chang, H. W. Li, S. C. Chen, J. Lu, and Y. Shi, *Appl. Phys. Lett.* **94**, 162111 (2009).
- ²¹K. C. Chang, T. M. Tsai, T. C. Chang, Y. E. Syu, C.-C. Wang, S. K. Liu, S. L. Chuang, C. H. Li, D. S. Gan, and S. M. Sze, *Appl. Phys. Lett.* **99**(26), 263501 (2011).
- ²²T. M. Tsai, K. C. Chang, T. C. Chang, G. W. Chang, Y. E. Syu, Y. T. Su, G. R. Liu, K. H. Liao, M. C. Chen, H. C. Huang *et al.*, *IEEE Electron Device Lett.* **33**(12), 1693–1695 (2012).
- ²³T. Y. Tseng and H. Nalwa, *Hand Book of Nanoceramics and their Based Nano Devices* (American Scientific Publishers, USA, 2009), pp. 175–176.
- ²⁴R. Waser, R. Dittmann, G. Staikov, and K. Szot, *Adv. Mater.* **21**, 2632–2663 (2009).
- ²⁵S. Takagi, A. Toriumi, M. Iwase, and H. Tango, *IEEE Trans. Electron Devices* **41**(12), 2357–2362 (1994).